Title
Detecting radiation reaction at moderate laser intensities:

Journal
Physical Review E, 91(2)

ISSN
1539-3755

Authors
Heinzl, Thomas
Harvey, Chris
Ilderton, Anton
et al.

Publication Date
2015-02-01

Detecting radiation reaction at moderate laser intensities **

Thomas Heinzl,[1,*] Chris Harvey,[2] Anton Ilderton,[3] Mattias Marklund,[3,4] Stepan S. Bulanov,[5] Sergey Rykovanov,[6] Carl B. Schroeder,[6] Eric Esarey,[6] and Wim P. Leemans[6]

[1]*School of Computing and Mathematics, Plymouth University, Plymouth PL4 8AA, UK*
[2]*Centre for Plasma Physics, Queen's University Belfast, BT7 1NN, UK*
[3]*Department of Applied Physics, Chalmers University of Technology, SE-41296 Gothenburg, Sweden*
[4]*Department of Physics, Umeå University, SE-901 87 Umeå, Sweden*
[5]*University of California, Berkeley, California 94720, USA*
[6]*Lawrence Berkeley National Laboratory, Berkeley, California 94720, USA*

We propose a new method of detecting radiation reaction effects in the motion of particles subjected to laser pulses of moderate intensity and long duration. The effect becomes sizeable for particles that gain almost no energy through the interaction with the laser pulse. Hence, there are regions of parameter space in which radiation reaction is actually the dominant influence on charged particle motion.

I. INTRODUCTION

In a conceptually simple experiment [1] it was shown that electron motion in a sufficiently intense laser becomes relativistic. In that experiment, a laser pulse was used to ionise a target gas, liberating electrons. After the electrons left the pulse, their energies and ejection angle were measured. Different values for these variables are predicted by relativistic and non-relativistic equations of motion; the experiment supported the relativistic prediction. (The phrase 'mass shift' in [1] refers to the 'relativistic mass' $m\gamma$; the experiment was not concerned with, and did not observe, the intensity dependent mass shift, for which see [2].)

In this paper we propose a similar experiment to measure classical radiation reaction (RR). The problem of RR on the dynamics of charged particles in electromagnetic (EM) fields is long standing, and has attracted a great deal of attention for more than a century (see [3, 4] for recent overviews). It is relevant for charged particle acceleration in terrestrial laboratories and in ultra-high energy cosmic rays. The interaction of charged particles with laser radiation provides special conditions for studying not only the interaction itself, but also RR effects. Present day PW-class laser facilities, such as BELLA [5], are at the threshold of the interaction regime dominated by RR effects, which are potentially able to completely change the nature of charged particle interactions with EM fields [6, 7].

The idea of this paper is simple: an experiment very similar to that in [1] is performed, and the properties of the emitted electrons measured. These are then used to test the predictions of the classical equations of motion with and without RR. There is no need to measure the properties of the produced radiation. This is good news in view of the recent finding (for a different interaction set-up) that RR effects are almost invisible in the radiation spectrum while they are more than obvious in the electron distribution [8]. This difference in size is consistent with the fact that RR effects are suppressed in the photon spectrum (by a factor of the classical RR parameter, see below) relative to those in the electron spectrum [9].

We argue that there exists, in the parameter space of interactions between a particle and a moderately intense laser pulse, a region in which the final state of the particle is determined almost entirely by RR effects. Moreover, in some special cases, the difference between the results which account for RR and those that neglect it, can serve as an unambiguous observable of the presence of RR effects.

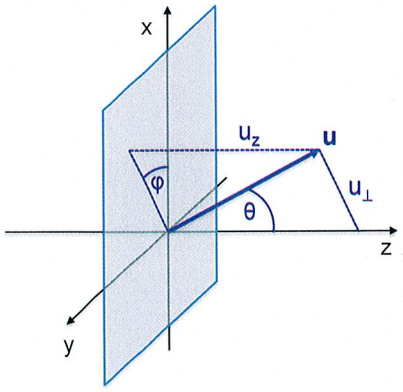

FIG. 1. Sketch of the ejection geometry with the laser propagating in z direction. θ and φ are polar and azimuthal ejection angles, respectively. $\mathbf{u}$ denotes the spatial part of the electron four-velocity.

II. REVIEW

Let the laser propagate along the z-axis (see Fig. 1). The polar and azimuthal electron ejection angles, relative to this axis, are $\theta \in [0, \pi]$, $\varphi \in [0, 2\pi]$ respectively. They are determined by the following electron velocity ratios at large times, i.e. after the pulse has passed ($\perp = \{x, y\}$),

$$\tan\varphi = \frac{u_y}{u_x}\,, \qquad \tan\theta = \frac{|u_\perp|}{u_z}\,. \tag{1}$$

As usual (see e.g. the text [10]) the u_i denote four-velocity components and $u_\perp = (u_x^2 + u_y^2)^{1/2}$. In the original experiment [1], the polar angle measurement was accompanied by

* theinzl@plymouth.ac.uk

** This work was supported by the Director, Office of Science, Office of High Energy Physics, of the U.S. Department of Energy under Contract No. DE-AC02-05CH11231.

a determination of the electron energy, i.e. its gamma factor, $\gamma = E_p/m$, the ratio of electron energy, E_p, and mass, m (in relativistic units, $c = 1$). The laser had a pulse duration of 1 ps and a peak intensity of approximately 10^{18} W/cm^2. The experimental results were compared against the theoretical analysis of [1] which assumed the laser to be a pulsed plane wave. For propagation along the z-axis, the plane wave depends solely on the invariant phase $\phi := k\cdot x$, with light-like laser four-momentum $k^\mu = \omega(1,0,0,1) \equiv \omega n^\mu$, and ω a typical value in the frequency spectrum of the pulse. For a charge e, moving in a plane EM wave with four-velocity $u^\mu = (\gamma, u_x, u_y, u_z)$, the light-front component $nu = \gamma - u_z \equiv u^-$ is conserved [11–13], as is the transverse canonical momentum [14]. This allows the remaining component u^+ to be determined by the mass-shell condition. In other words, the existence of three momentum conservation laws, together with the mass-shell condition, means the dynamics is integrable.

Let the pulse extend over the phase interval $\phi_1 \le \phi \le \phi_2$, and let a free electron 'appear' in the pulse at phase ϕ_i, with velocity u_i, following ionisation (the mechanism for which will be discussed below). The subsequent velocity of the charge then assumes the compact form

$$u^\mu = u_\mathrm{i}^\mu - a^\mu + (u_\mathrm{i}\cdot a - a^2/2)\,\frac{n^\mu}{n\cdot u}\,, \tag{2}$$

in which dimensionless a^μ is the phase integral of the (transverse) electric field $E^\mu \equiv (0, \mathbf{E}_\perp, 0)$,

$$a^\mu(\phi_\mathrm{i};\phi) = \int_{\phi_\mathrm{i}}^{\phi} \mathrm{d}\varphi\, \frac{eE^\mu(\varphi)}{m\omega}\,. \tag{3}$$

We refer to this as the potential [15]. Note that the integral is taken from the phase value ϕ_i at ionisation onwards. We will henceforth assume, as in [1], that the electron is at rest immediately post-ionisation. This is a natural approximation for ionisation by a linearly polarised EM wave [16]. Adopting relativistic units ($c = 1$) we have $u_\mathrm{i}^\mu = (1,0,0,0)$, whence $u_\mathrm{i}\cdot a = 0$ and $n\cdot u = 1$. Plugging this into (2) yields the velocity components appearing in (1),

$$\mathbf{u}_\perp = -\boldsymbol{a}_\perp\,, \tag{4}$$

$$u_z = -a_\perp^2/2\,. \tag{5}$$

The first identity states the conservation of canonical momentum, rewritten in our condensed notation. It says that the transverse motion is harmonic, following the field oscillations in linear response at frequency ω, with a maximum excursion per cycle given by $a_\perp\lambda$, where $\lambda = 2\pi/\omega$. The longitudinal velocity, u_z, however, is quadratic in the potential, hence includes the first harmonic at frequency 2ω. This results in the well known Lissajous figure-8 motion (in the average rest frame, assuming linear polarisation).

Plugging (4) and (5 into (1) one finds that the polar emission angle $\theta(\phi_\mathrm{i};\phi_2)$, evaluated at the final phase $\phi = \phi_2$ marking the end of the pulse, obeys

$$\tan\theta\,(\phi_\mathrm{i};\phi_2) = \frac{2}{|a_\perp(\phi_\mathrm{i};\phi_2)|}\,, \tag{6}$$

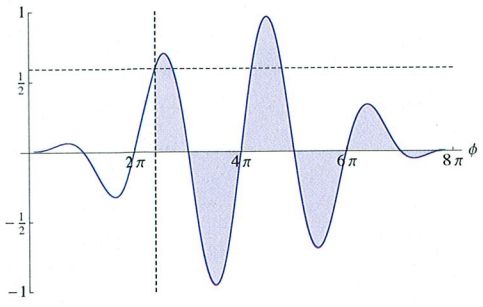

FIG. 2. Sketch of the field of a laser pulse. The horizontal dashed line represents the ionisation threshold. Only the shaded region contributes to the integral (3) determining the electron ejection angle.

provided that $a(\phi_\mathrm{i};\phi_2) \neq 0$ and that this is correlated with the final gamma factor by

$$\tan^2\theta\,(\phi_\mathrm{i};\phi_2) = \frac{2}{\gamma(\phi_\mathrm{i};\phi_2) - 1}\,, \tag{7}$$

provided that final $\gamma > 1$, see below. This parametric relation was tested and confirmed in [1], for a variety of noble gas targets with different ionisation thresholds giving different ionisation times ϕ_i.

From (7), the ejection angle measures the energy transfer to the electron in a plane wave. That this is non-zero does not contradict the Lawson-Woodward theorem [17–19]. The loophole is that the electrons do not see the whole pulse; they are bound in atoms until the pulse amplitude exceeds the ionisation threshold, at which point, ϕ_i, they are injected into the pulse, see Fig. 2. The energy transfer predicted in (7) and confirmed in [1] is therefore an example of ionisation induced sub-cycle acceleration [20, 21]. Note that an electron, experiencing the passing of the *whole* pulse, would in total have gained zero energy and momentum because $a(\phi_1;\phi_2) = 0$, assuming the background has no DC-component [22]. As a consequence, the tangent in (6) and (7) becomes infinite, seemingly implying that free electrons experiencing the full duration ($\phi_\mathrm{i} \to \phi_1$) of a pulsed plane wave should be ejected orthogonally to the beam. This is misleading though; in deriving (6) (and already in (1)) we have assumed the particle has a nonzero velocity. While particles which come to rest after leaving the pulse will be displaced from their original positions, they would not be detected by a distant detector, and so will not be considered further here.

III. RADIATION REACTION

The Lorentz-Abraham-Dirac (LAD) equation [23–25] may be compactly written as

$$m\dot{u}^\mu = \frac{e}{c}F^{\mu\nu}u_\nu + \tau_0 m\,\mathbb{P}^{\mu\nu}\ddot{u}_\nu\,, \tag{8}$$

with the projection $\mathbb{P}^{\mu\nu} = g^{\mu\nu} - u^\mu u^\nu$ guaranteeing $u^2 = 1$. Hence, the Lorentz force term containing the field strength

$F^{\mu\nu}$ is augmented by RR terms that are multiplied by the purely classical time parameter (temporarily reinstating the speed of light, c)

$$\tau_0 := \frac{2}{3}\frac{r_e}{c} = \frac{2}{3}\alpha\frac{\lambda\!\!\!^{-}_e}{c} = \frac{e^2}{6\pi mc^3} \simeq 2\ \mathrm{fm}/c\ , \tag{9}$$

r_e denoting the classical electron radius, $\alpha = e^2/4\pi\hbar c \simeq 1/137$ the fine structure constant and $\lambda\!\!\!^{-}_e$ the Compton wavelength of the electron. A dimensionless parameter $\epsilon_{\rm rad}$ characterising RR may be obtained by taking the ratio of τ_0 to the typical time scale of the laser, $1/\omega$:

$$\epsilon_{\rm rad} := \omega\tau_0 = \frac{2}{3}\frac{r_e}{\lambda\!\!\!^{-}} = \frac{2}{3}\alpha\frac{\hbar\omega}{mc^2}, \tag{10}$$

with $\lambda\!\!\!^{-}$ the (reduced) laser wavelength. A precursor of this parameter was already introduced by Lorentz [23] (see again the useful overview article [3]), and Koga et al. emphasised its importance in a discussion of RR corrections to nonlinear Thomson scattering [27]. When $\epsilon_{\rm rad}$ approaches unity one reaches a regime where the RR force is of the same magnitude as the Lorentz force, but as $\hbar\omega \simeq 200\, mc^2$ in this case, one has simultaneously entered the quantum regime [28].

In this paper we will treat RR as a correction to the Lorentz force effects, i.e. we will work to first order in $\epsilon_{\rm rad}$. With this restriction one can replace the $m\dot{u}$ term in (9) by the time derivative of the Lorentz force, an iteration that results in the Landau-Lifshitz (LL) equation [10]. (See [29, 30] for recent comparisons of LAD and LL equations, and [31] for higher order corrections.) We can therefore appeal to the known analytic solution of the Landau-Lifshitz equation in a plane wave [32], and then truncate to order $\epsilon_{\rm rad}$. The $\mathcal{O}(\epsilon_{\rm rad})$ expressions are not illuminating, so for simplicity we recall here the exact solution, which may be written akin to the Lorentz solution (2). Following [32], and abbreviating the derivative with respect to phase ϕ by $a' \equiv eE/m\omega$, cf. (3), we introduce the auxiliary function

$$h(\phi_{\rm i};\phi) = 1 - \epsilon_{\rm rad}\int_{\phi_{\rm i}}^{\phi} \mathrm{d}\varphi\, a'^2\ . \tag{11}$$

This parameterises the main dynamical effect of RR on a particle in a plane wave, namely that u^- ceases to be conserved [12, 13]. Instead, one has

$$u^-(\phi_{\rm i};\phi) = u^-_{\rm i}/h(\phi_{\rm i};\phi)\ , \tag{12}$$

which is monotonically decreasing. For a particle initially at rest the solution of the Landau-Lifshitz equation assumes the compact form

$$v^\mu := hu^\mu = u^\mu_{\rm i} - \mathcal{A}^\mu + \left[-\tfrac{1}{2}\mathcal{A}^2 + \tfrac{1}{2}(h^2-1)\right]\frac{n^\mu}{n\cdot u}\ , \tag{13}$$

which replaces (2) by utilising the modified potential

$$\mathcal{A}^\mu := \int_{\phi_{\rm i}}^{\phi} \mathrm{d}\varphi\,(ha'^\mu + \epsilon_{\rm rad}a''^\mu)\ , \tag{14}$$

where, again, primes denote derivatives with respect to elapsed phase, ϕ. As required by consistency, $\mathcal{A} \to a$ in the absence of RR, i.e. when $\epsilon_{\rm rad} \to 0$. The essential point of this paper is simply that the predictions of (11)-(14) are quantitatively different from those of (2). For example, a particle initially at rest which is struck by a plane wave can gain energy and momentum from the wave, as discussed in [13, 33]. It follows that an experiment like that in [1] can, in principle, be used to detect RR effects.

It is convenient here to factorise the electric field into amplitude, shape and polarisation. We therefore define the dimensionless laser amplitude, a_0, in terms of the peak value, $E_{\rm peak}$, of the laser electric field, as

$$a_0 = eE_{\rm peak}/m\omega\ , \tag{15}$$

shape functions $f_i(\phi)$ and transverse polarisation vectors ϵ^μ_i obeying $\epsilon_i\cdot\epsilon_j = -\delta_{ij}$. The field strength is then

$$eE^\mu/m\omega = a_0\, f_i(\phi)\,\epsilon^\mu_i = a'^\mu\ . \tag{16}$$

With this, the RR correction function h defined in (11) can be written in the form

$$h = 1 + \epsilon_{\rm rad}\, a_0^2\, F_{ii}\ , \tag{17}$$

where we have defined the dimensionless integral

$$F_{jj}(\phi) := \int_{\phi_{\rm i}}^{\phi} \mathrm{d}\varphi\, f_j(\varphi) f_j(\varphi)\ , \tag{18}$$

(sum over j on the RHS) which is of order *at most* the pulse duration in ϕ, i.e.

$$0 \le F_{jj} \le (\phi_2 - \phi_1) =: 2\pi N\ . \tag{19}$$

Here, N denotes the number of cycles in the pulse, so we can approximate $F_{jj} \sim O(N)$. The important parameter inferred from (17) is therefore [34]

$$\epsilon_{\rm rad} a_0^2 N\ , \tag{20}$$

which suggests that one can compensate for the smallness of α and ω/m in (10) by using high intensity and/or long pulses [35]. The regime dominated by purely classical RR without quantum 'contamination' is defined by the inequality $\epsilon_{\rm rad} \ll \epsilon_{\rm rad} a_0^2 \simeq 1$.

To be explicit we again consider the ratio of transverse and longitudinal velocities, cf. (1),

$$\tan\theta_{\rm RR} := \frac{u_\perp}{u_z} = \frac{v_\perp}{v_z}\ , \quad v_\perp = (v_j v_j)^{1/2}\ . \tag{21}$$

The RR modifications of the velocity components (4) and (5) are straightforwardly obtained from (13),

$$v_j = -\mathcal{A}_j\ , \tag{22}$$

$$v_z = -\frac{1}{2}(\mathcal{A}^2 - h^2 + 1)\ . \tag{23}$$

It is quite clear that these can be written as a sum of two contributions, the solution of the pure Lorentz force equation plus an RR correction,

$$v = v_{\rm L} + \epsilon_{\rm rad}\delta v \ , \quad v_{\rm L} \equiv u_{\rm L} \ . \tag{24}$$

Inserting this decomposition into (21) one obtains

$$\tan\theta_{\rm RR} = \frac{v_{{\rm L},\perp} + \epsilon_{\rm rad}\delta v_\perp}{v_{{\rm L},z} + \epsilon_{\rm rad}\delta v_z} \ . \tag{25}$$

Typically, one would expect the RR terms to represent a small correction to the leading Lorentz contribution,

$$\epsilon_{\rm rad}\delta v \ll v_{\rm L} = u_{\rm L} \ , \tag{26}$$

and expand (25) in $\epsilon_{\rm rad}$,

$$\tan\theta_{\rm RR} = \tan\theta_{\rm L}\left\{1 + \epsilon_{\rm rad}\left(\frac{\delta v_\perp}{v_{{\rm L},\perp}} - \frac{\delta v_z}{v_{{\rm L},z}}\right)\right\} \ , \tag{27}$$

with $\tan\theta_{\rm L} := u_{{\rm L},\perp}/u_{{\rm L},z}$. However, if one were able to identify a parameter regime where the leading contributions vanish, such that the RR terms would dominate, $\epsilon_{\rm rad}\delta v \gg v_{\rm L}$, the result for the ejection angle would be quite different,

$$\tan\theta_{\rm RR} = \frac{\delta v_\perp}{\delta v_z} \ . \tag{28}$$

Note in particular that this observable characterises the strength of RR effects, but is independent of $\epsilon_{\rm rad}$.

To see whether the scenario with RR dominance can be realised we have to evaluate the velocity v in terms of laser parameters and pulse shapes. It will be convenient to define a pulse integral "seen" by the ionised electrons after ionisation time, $\phi_{\rm i}$,

$$\langle\ldots\rangle_{\rm i2} := \int_{\phi_{\rm i}}^{\phi_2} d\phi \ldots \ . \tag{29}$$

and the auxiliary integral functions generalising (18)

$$F_{i_1 i_2 \ldots i_n}(\phi_{\rm i},\phi) := \int_{\phi_{\rm i}}^{\phi} d\varphi\, f_{i_1} f_{i_2} \ldots f_{i_n} \ . \tag{30}$$

For linear polarisation, we just count the power of f in the integrand,

$$F_n(\phi) := \int_{\phi_{\rm i}}^{\phi} d\varphi\, f^n(\varphi) \ . \tag{31}$$

Hence, $F'_{i_1 i_2 \ldots} = f_{i_1} f_{i_2} \ldots$ and $F'_n = f^n$.

Plugging the parameterisation (16) into (13) and employing the new notation the velocity components (22) and (23) decompose into the Lorentz contributions

$$v_j = u_j = -a_0\langle f_j\rangle_{\rm i2} \ , \tag{32}$$

$$v_z = u_z = \tfrac{1}{2}a_0^2\langle f\rangle_{\rm i2}^2 \ , \tag{33}$$

and the RR terms

$$\delta v_j = -a_0\{\langle F'_j\rangle_{\rm i2} + a_0^2\langle f_j F_{ii}\rangle_{\rm i2}\} \ , \tag{34}$$

$$\delta v_z = a_0^2\Big\{\langle f_i\rangle_{\rm i2}\langle F'_i\rangle_{\rm i2} + \langle f^2\rangle_{\rm i2} + a_0^2\langle f_j\rangle_{\rm i2}\langle f_j F_{ii}\rangle_{\rm i2}\Big\} \ , \tag{35}$$

where we have abbreviated $\langle f\rangle_{\rm i2}^2 := \langle f_i\rangle_{\rm i2}\langle f_i\rangle_{\rm i2}$, summing over repeated indices.

As expected, the right-hand sides in (34) and (35) involve the laser amplitude a_0, the RR parameter $\epsilon_{\rm rad}$ and integrals over up to three pulse shape functions f_j. Of course, the δv's are *parametrically* small: if we send $\epsilon_{\rm rad} \to 0$ (no RR at all) we recover (6), which takes the form

$$\tan\theta_{\rm L}(\phi_{\rm i},\phi_2) = \frac{2}{a_0\langle f\rangle_{\rm i2}} \ . \tag{36}$$

Assuming that the inequality (26) holds, so that (34) and (35) are indeed small corrections to the Lorentz terms, we find that (27) turns into

$$\frac{\tan\theta_{\rm RR}}{\tan\theta_{\rm L}} - 1 = -\frac{\epsilon_{\rm rad}}{\langle f\rangle_{\rm i2}^2}\Big(\langle f_i\rangle_{\rm i2}\langle F'_i\rangle_{\rm i2} + 2\langle f^2\rangle_{\rm i2} + a_0^2\langle f_i\rangle_{\rm i2}\langle f_i F_{jj}\rangle_{\rm i2}\Big) \ , \tag{37}$$

correct to order $\epsilon_{\rm rad}$. For large $a_0 \gg 1$ the last term dominates and we have the simple result

$$\frac{\tan\theta_{\rm RR}}{\tan\theta_{\rm L}} - 1 = -\epsilon_{\rm rad}a_0^2\langle f_i\rangle_{\rm i2}\langle f_i F_{jj}\rangle_{\rm i2}/\langle f\rangle_{\rm i2}^2 \ . \tag{38}$$

The crucial question now is whether there is a regime with RR dominance where the inequality (26) is violated. The simplest realisation of this scenario is provided if the Lorentz terms (32) and (33) were zero (or very nearly so). As these are entirely determined by the pulse integral, $\langle f\rangle_{\rm i2}$, we need the latter to be zero:

$$\langle f\rangle_{\rm i2} = 0 \ . \tag{39}$$

Due to the oscillatory nature of the EM field the solutions to this equation are a set of $\phi_{\rm i}$ distributed over the duration of the laser pulse. In most cases, however, the initial phase interval for which the inequality $\epsilon_{\rm rad}\delta v \gg u_{\rm L}$ is satisfied is negligibly small. Only in the limit $\phi_{\rm i} \to \phi_1$, i.e. when the pulse integral extends over the *total* pulse duration, $\phi_1 \le \phi \le \phi_2$, does the interval become large. In the strict limit, the electrons will need to be present just before the pulse arrives, hence will need to be ionised by means different from the pulse itself (see below). As a consequence, these electrons will 'see' the whole pulse which integrates to zero. In the absence of RR they will gain no energy from the interaction with the pulse, as dictated by the Lawson-Woodward theorem. On the other hand, when RR is taken into account, it will provide the *leading* contribution to the final energy of the electrons. This will remain true even for $\phi_{\rm i} > 0$ as long as RR dominance holds, $\epsilon_{\rm rad}\delta v \ge u_{\rm L}$. To analyse what is happening we note that the late-time integral from $\phi_{\rm i}$ to ϕ_2 is minus the early-time integral from ϕ_1 to

ϕ_i. This latter integral may be Taylor expanded,

$$\int_{\phi_1}^{\phi_i} d\phi\, f(\phi) =: \sum_{l=l_0}^{\infty} \phi_i^{l+1} f^{(l)}(\phi_1)\ , \tag{40}$$

which tells us that the short-time asymptotics of the Lorentz terms (32) and (33) is basically determined by the first non-vanishing derivative, $f^{(l_0)}$, at the beginning ϕ_1 of the pulse. This suggest using pulses with a rather steep rise. The limiting values ($\phi_i \to \phi_1$) for the velocity components from (34) and (35) are obtained by setting $\langle f_j\rangle_{12} = \langle F'_j\rangle_{12} = 0$,

$$\delta v_j(\phi_1,\phi_2) = -\epsilon_{\rm rad} a_0^3 \langle f_j F_{ii}\rangle_{12}\ , \tag{41}$$

$$\delta v_z(\phi_1,\phi_2) = \epsilon_{\rm rad} a_0^2 \langle f^2\rangle_{12}\ . \tag{42}$$

Taking their ratio according to (28) results in the limit

$$\tan\theta_{\rm as}(\phi_1,\phi_2) = a_0 \frac{\left(\langle f_j F_{ii}\rangle_{12}\langle f_j F_{kk}\rangle_{12}\right)^{1/2}}{\langle f^2\rangle_{12}}\ , \tag{43}$$

where we have defined $\theta_{\rm as} := \theta_{\rm RR}(\phi_1,\phi_2)$. For $\phi_i > \phi_1$ there will be corrections to (43), which, in principle, can be determined via the expansion (40). It is simpler, though, to discuss a few examples numerically. This is the topic of the next section.

IV. EXAMPLES

A. Pulses with compact support

We choose linear polarisation ($f_1 = f, f_2 = 0$) and a sinusoidal envelope of compact support [36, 37] and duration $2\pi N$,

$$f(\phi) = \sin^K(\phi/2N)\sin(\phi)\ ,\quad 0 \le \phi \le 2\pi N\ . \tag{44}$$

The integer N counts the number of cycles in the pulse, while the integer K determines the shape of the envelope. Typically, one chooses K to be even and not too large ($K = 2$ or $K = 4$). Note that the pulse rises like ϕ^{K+1} at its front ($\phi \ll 1$), so the first nonvanishing derivative will be $f^{(K+1)}(0)$, cf. (40), so that

$$\langle f\rangle_{i2} \sim \phi_i^{K+2}\ . \tag{45}$$

Before we enter a detailed numerical discussion let us try to get an idea of what is going on by considering the asymptotic ejection angle $\theta(\phi_1,\phi_2)$. For linear polarisation, (43) immediately simplifies to

$$\tan\theta_{\rm as} = a_0 \frac{\langle f F_2\rangle_{12}}{\langle f^2\rangle_{12}} = -a_0 \frac{\langle f^2 F_1\rangle_{12}}{\langle f^2\rangle_{12}}\ . \tag{46}$$

We are interested in the dependence of this angle on pulse duration, N keeping K fixed. The result for $K = 2$ is shown in Fig. 3, from which one can identify two regimes, small N and large N, i.e. short and long pulse duration, respectively. The behaviour of the graph is basically determined from the numerator $\langle f F_2\rangle_{12}$ in (46) via Fourier analysis. Defining a rescaled phase $\alpha := \phi/2N$, the Fourier spectrum of the pulse (44), viewed as a function of α, contains two distinct types of modes: there are modes of order $n \sim K$ from the envelope, and modes of order N corresponding to the laser carrier frequency, $\phi = 2N\alpha$. For small $N \sim K$, the modes of envelope and carrier wave interact, resulting in the oscillations at small N in Fig. 3. For long pulses, $N \gg K$, this cannot happen (N and K modes are orthogonal), which yields the tail behaviour of the graph. The latter can be determined analytically by evaluating (46) for the envelope (44), which results in

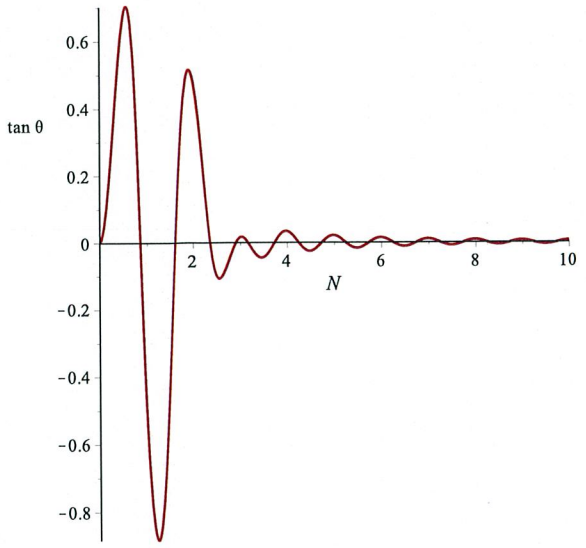

FIG. 3. $\tan\theta_{\rm as}$ from (46) as a function of pulse duration N for $K = 2$ and $a_0 = 2$. [Note that in the absence of RR this tangent would be infinite for any N as the asymptotic emission angle is $\pi/2$ in this case, cf. Fig. 11 below.]

$$\tan\theta_{\rm as} = \frac{a_0}{2(N^2-1)}\ ,\quad (N > 3)\ . \tag{47}$$

For $K = 4$ the situation is quite similar, with the tail behaviour given by

$$\tan\theta_{\rm as} = -\frac{3a_0}{2(N^2-4)(N^2-1)}\ ,\quad (N > 6)\ . \tag{48}$$

Thus, for large N (long pulses), the asymptotic emission angle goes to zero like a negative integer power of N as can be seen from Fig. 4, for $a_0 = 5$ and $a_0 = 50$, roughly corresponding to laser powers of 100 TW and 1 PW, respectively. In what follows we will focus on long pulses first.

To be specific, we choose the parameters of [38]: $a_0 = 10$, $N = 1600$ and $K = 2$, respectively corresponding to an intensity of $\sim 10^{20}$ W/cm^2, a total pulse duration of ~ 4 ps at optical frequency $\omega \sim 1$ eV, and a $\sin^2$ envelope. The results are shown in Fig. 5; for linear polarisation, the problem is planar and therefore we plot the angle $\theta_{xz} = \arctan(u_x/u_z)$ from the positive ($\theta_{xz} = \pi/2$) to negative ($-\pi/2$) x-axis. In

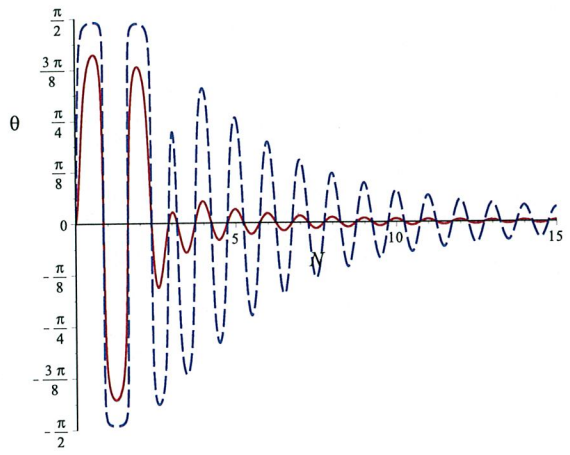

FIG. 4. Emission angle $\theta_{\rm RR}$ as a function of pulse duration N for $K = 2$ and $a_0 = 5$ (red/solid) and $a_0 = 50$ (blue/dashed).

the Lorentz case, for small $\phi_{\rm i}$, the emission direction is almost transverse to the laser, with a small u_z component, so $\theta_{xz} \sim \pm\pi/2$, with the jumps corresponding to the transverse velocity u_x changing sign while u_z stays small and positive. (This is the reason for plotting θ_{xz} instead of θ; it allows us to keep track of these sign changes.) For injection times within the first few cycles of the pulse, RR can give a change in angle as large as 90°. The difference between the Lorentz and RR prediction increases with *decreasing* injection time, so that RR effects are most significant for electrons released in the earliest part of the pulse.

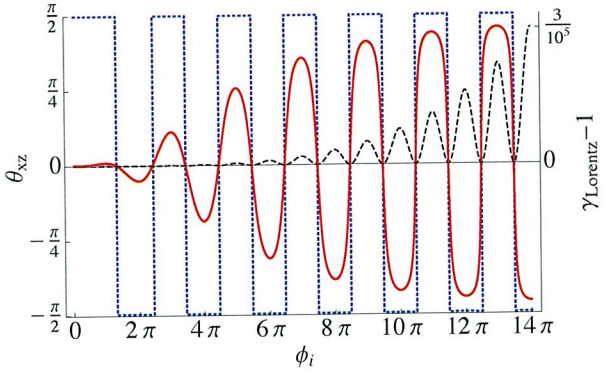

FIG. 5. *Left scale*: planar angle θ_{xz} for $N = 1600$, $a_0 = 10$, $\sin^2$ envelope, as a function of ionisation time $\phi_{\rm i}$, for Lorentz (blue/dotted) and RR (red/solid). *Right*: final Lorentz force gamma for the emitted particles (black/dashed).

Fig. 5 shows that the difference in emission angle is most significant for those particles which exit the pulse with the least energy; for the $\phi_{\rm i}$ in Fig. 5, we find that the final gamma factor with RR differs from unity by one part in $\mathcal{O}(10^5)$, and differs from the Lorentz force gamma by one part in $\mathcal{O}(10^7)$. Therefore, a clean environment would be desirable in order to avoid the deflection of these electrons before being detected.

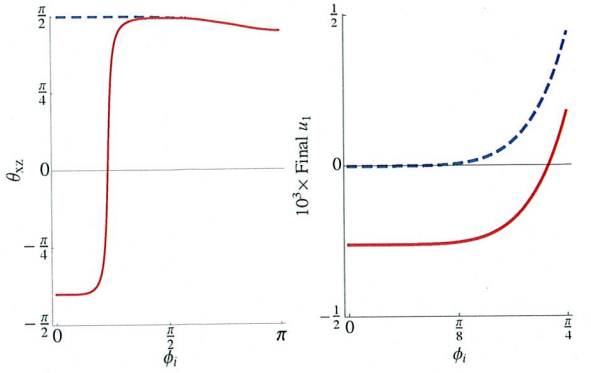

FIG. 6. *Left*: Planar angle θ_{xz}, for $N = 4$ cycles of an $a_0 = 50$ pulse with $\sin^4$ envelope. *Right*: final transverse velocity, as a function of $\phi_{\rm i}$. The sign flip in the transverse component, for $\phi_{\rm i} \lesssim \pi/4$, is responsible for the large change in emission angle. Blue/dashed: Lorentz case; Red/solid: RR.

The larger the difference in emission angle, the more easily observed would be the effect of RR. The extreme case is naturally that in which the angle is rotated by 180°, i.e. the emission direction is reversed. For *long* pulses, though, such a drastic reversal is absent: In Fig. 5, for a pulse of $N = 1600$ cycles, the transverse Lorentz and RR velocities change sign (hence reversal of emission) at the same phases.

For *short* pulses, however, RR effects can indeed cause emission reversal with respect to the pure Lorentz case. In this case the angle $\theta_{xz} \simeq \pi/2$ of the Lorentz case changes to $\theta_{xz} \simeq -\pi/2$ in the RR case; in other words, a particle which would emerge travelling slowly in the positive x-direction according to Lorentz, should emerge travelling slowly in the negative x-direction according to RR, a 180° change in direction. To provide a concrete example, we take a short pulse with laser parameters $N = 4$, $K = 4$ and $a_0 = 50$. Given the discussion above, this example should not be expected to match a realistic short, focussed pulse, but it is nevertheless interesting to look at the physics involved.

The emission angle θ_{xz} is plotted in the left panel of Fig. 6. For electrons released early in the first cycle, we see the almost 180° change in emission direction due to RR. This is because, for $\phi_{\rm i} \lesssim \pi/4$, RR causes a sign flip in the transverse velocity u_x (while u_z has the same sign with or without RR) see the second panel of Fig. 6. Note in particular that the RR contribution to the velocity components clearly *dominates* the Lorentz force contribution, which is very small compared to its RR counterpart: expanding the ratio of transverse components (with and without RR) for small initial angle ϕ_i, we find for the pulse (44)

$$|u_x(\text{Lorentz})/u_x(\text{RR})| \sim \phi_{\rm i}^6\,, \quad \phi_{\rm i} \ll 1\,. \tag{49}$$

Thus, for an initial phase of, say, $\phi_{\rm i} = 0.1$, the RR value for u_x will exceed the Lorentz value by six orders of magnitude. A qualitative sketch of the situation, showing the reversal of emission direction, is provided in Fig. 7.

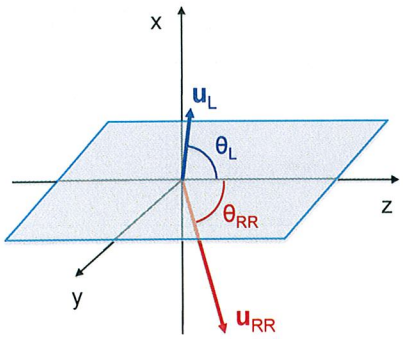

FIG. 7. Qualitative sketch (not to scale) of the reversal in ejection direction due to RR (red, subscript RR) as compared to the Lorentz case (blue, subscript L).

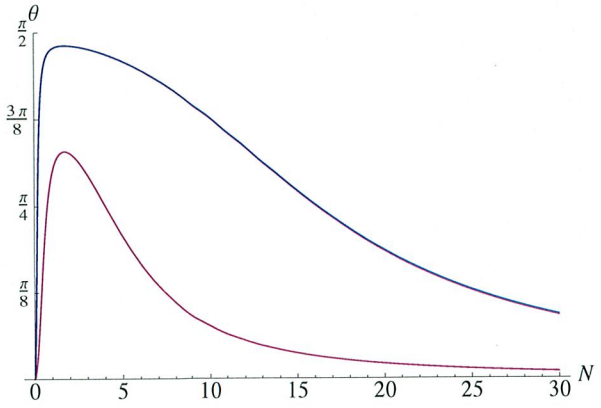

FIG. 8. $\theta_{\rm as}$ from (51) as a function of pulse duration N for the pulse (50). Upper curve: $a_0 = 50$, lower curve: $a_0 = 5$.

The behaviour of RR dominance displayed in Fig. 6 and Fig. 7 represents a dramatic deviation from the Lorentz force. It occurs for electrons created very early in the pulse, i.e. when ionisation takes place at $\phi_{\rm i}$ near zero. (The realisation of such an early ionisation will be discussed further below.)

B. Pulses with exponential envelope

In order to study the influence of the pulse shape we want to consider another example of an analytically tractable pulse [39], namely

$$f(\phi) = \exp(-|\phi|/N)\sin\phi\ , \quad -\infty < \phi < \infty\ . \tag{50}$$

The exponential envelope is not differentiable at $\phi = 0$, but as the sine is vanishing there, the pulse remains smooth. Again, we first consider the asymptotic RR emission angle, $\theta_{\rm as}$, i.e. $\theta_{\rm RR}$ evaluated for $\phi_{\rm i} \to -\infty$. The analytic result for the pulse (50) is

$$\tan\theta_{\rm as} = \frac{16a_0}{3}\,\frac{N^2}{(N^2+9)(N^2+1)}\ , \tag{51}$$

which goes like $1/N^2$ for large N.

In Fig. 8 we plot (51) as a function of pulse duration, N, for moderate and large intensity ($a_0 = 5$ and $a_0 = 50$, respectively). Comparing with Fig. 4, one again finds a maximum for small $N \simeq 3$, though no oscillations, and a power-law tail for large N. So, as with the pulse (44), one might expect the small-N and large-N behaviour to be qualitatively different. Numerically, this expectation turns out not to be true. The shape of θ as a function of ionisation phase seems to be rather independent of both N and a_0. For larger intensities, however, the maximum at small N increases towards $\pi/2$.

We next discuss the dependence of the emission angle on ionisation phase, $\phi_{\rm i}$, beginning with a short pulse ($N = 4$) of moderate intensity ($a_0 = 5$). In Fig. 9 we display the associated emission angles $\theta_{\rm L}$ and $\theta_{\rm RR}$. While the former oscillates between $-\pi/2$ and $\pi/2$ as in Fig. 5, RR forces the emission angle to approach these oscillations smoothly with increasing $\phi_{\rm i}$, starting from a nonvanishing asymptotic value $\theta_{\rm as}$ given by (46). For $N = 4$ the asymptotic emission angle becomes

$$\theta_{\rm as} = \arctan(256/255) \simeq \pi/4\ , \tag{52}$$

as can be checked against Fig. 9, top panel. A rather similar behaviour is found for a long intense pulse with $N = 40$ and $a_0 = 50$. In this case, however, it takes many cycles for the oscillatory RR behaviour to approach the curve with RR absent, see Fig. 9, bottom panel. The asymptotic emission angle for $N = 40$ is $\theta_{\rm as} = 0.164$, which agrees with the value in the figure.

V. DISCUSSION

In the above we have identified observables where the total effects due to the Lorentz force cancel and *only* RR effects remain, an effect one may call *RR dominance*. This is not in contradiction to the assumption that RR effects are small: for the parameters in this paper one has $R \lesssim 10^{-3}$, and it is easily verified that RR contributions to the velocity components are subleading at each *instant* in time ('local' effects). However, RR dominance arises as an accumulative ('nonlocal') phenomenon: when integrating over only a part of the pulse, it is still possible for energy gains/losses due to the Lorentz force to vanish, while energy gains/losses due to RR do not.

It remains to discuss the question of ionisation early into the pulse. For the pulse (44) with the given parameters, the probability of optical ionisation at small $\phi_{\rm i}$ is well into the multiphoton regime and therefore negligibly small. Thus the injection of electrons must be achieved by some external source. We choose here to introduce a short, co-propagating X-ray pulse, that will ionise hydrogen at a specific ϕ_i. For multiphoton ionisation by an X-ray pulse it is plausible to expect that the momentum distribution will be extremely narrow with the maximum at zero momentum, so we can neglect this distribution and consider electrons born at rest. Moreover the effects of the X-ray pulse field on the ejection angle are negligible.

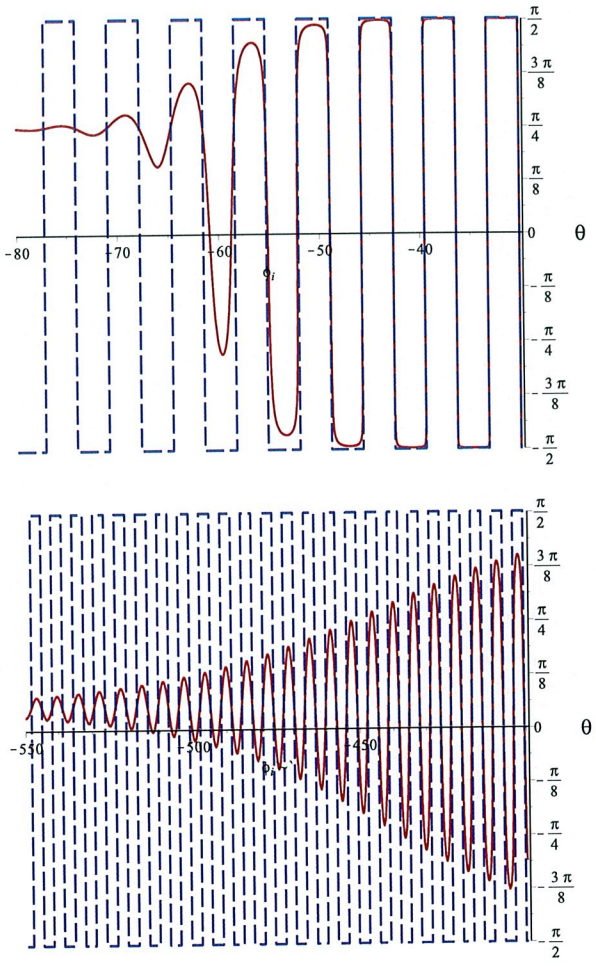

FIG. 9. $\theta_{\rm L}$ (blue/dashed) and $\theta_{\rm RR}$ (red/solid) as functions of ionisation phase $\phi_{\rm i}$ for the pulse (50) with (top panel) $N = 4$, $a_0 = 5$ and (bottom panel) $N = 40$ and $a_0 = 50$.

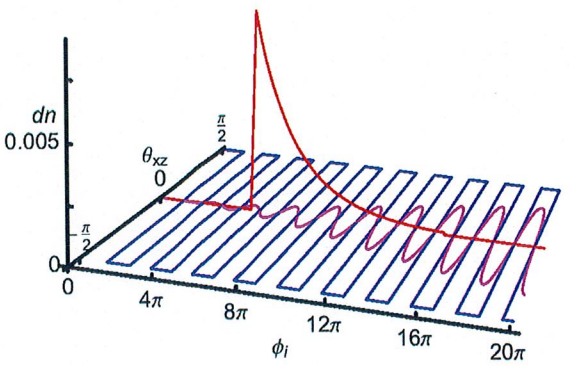

FIG. 10. *Horizontal plane:* Planar ejection angle θ_{xz} for $N = 1600$, $a_0 = 10$, $\sin^2$ envelope, as a function of ionisation time $\phi_{\rm i}$, for Lorentz (blue/rectangular) and RR (magenta/rounded). Note the difference in ejection angle between pure Lorentz and RR scenarios. *Vertical direction*: Ionisation rate dn as defined in the main text.

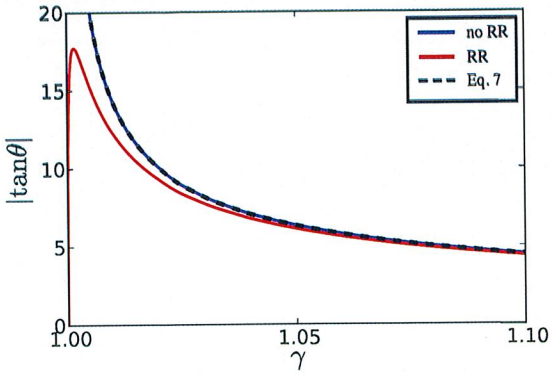

FIG. 11. Numerical result for the correlation between final emission angle and gamma, for $a_0 = 200$, $\sin^4$ envelope. Blue/top curve: Lorentz force, see [1]. Red: RR result. The black/dashed line corresponds to (7).

We took a 30 fs X-ray pulse with $\omega \sim 50$ eV and intensity 1.2×10^{15} W/cm^2. Such parameters were chosen to ensure total ionisation of hydrogen gas and its subsequent injection during the phase interval $\phi_{\rm i} \in [5\pi, 15\pi]$. For these phase values one is well in the region of RR dominance so that there are significant differences between Lorentz and RR predictions. To illustrate the situation we define an ionisation rate $dn := n'(\phi_{\rm i})/n_0 = w \exp(-w\phi_{\rm i})$ where the prime denotes a derivative with respect to the argument, n_0 the initial gas density and $w = \Gamma/\omega$ the one-photon ionisation rate Γ [40] in units of the laser frequency, ω. (Note that w is dimensionless.)

The associated ionisation rate dn and the ejection angle θ_{xz} are shown in Fig. 10 as a function of initial phase, $\phi_{\rm i}$.

Inspired by the successful experiment [1], and using the same plane wave model, we have identified a parameter regime in which RR effects are leading rather than subleading. We are aware, though, that numerical methods will be essential for extending the above to more refined models [41–45]. As a preparation for this, we have performed numerical simulations using the code PATRA [46]. For a given charged particle, the code solves the Landau-Lifshitz equation using a fourth order Runge-Kutta method. To mimic ionisation, each particle is assigned a certain unique value of the electric field amplitude, below which the particle is immobile. When the field exceeds this amplitude, the particle is 'injected' into the simulations (with zero velocity) and begins to move under the influence of the EM field. The code reproduces the first panel plot of Fig. 6 extremely well; the respective curves are on top of each other. In Fig. 11 we plot, using the code, the parametric relations between final gamma and emission angle. The blue (top) curve is the Lorentz result, as in (7) and [1]. The red curve shows the RR result, with the difference being greatest for smallest final gamma.

Since the RR signals studied here are most pronounced for

electrons leaving the pulse with low energies, the impact of residual Coulomb interactions between electrons should also be included in future, more comprehensive, simulations.

As for experimental realisation of the proposed scheme, external guiding structures and high-order modes for laser pulses [5, 44] can be used to counter diffraction of laser radiation and prevent ponderomotive scattering, ensuring the interaction of electrons with only the high intensity part of the laser pulse. Quite generally, the plane wave model should work as long as the maximal transverse excursion of the electron remains significantly smaller than the beam waist, $\lambda a_0 \ll w_0$. This could be realised by ensuring on-axis injection to sufficient accuracy and by using wide flat-top beams. In this way, the injected electrons would not "see" large field gradients.

VI. CONCLUSIONS

We have described a simple experiment which can be used to observe the effects of classical radiation reaction, without going to ultra-high intensities. The proposed experiment follows that in [1]. A target is ionised by a laser pulse, and the momentum components of the released electrons are measured, after they leave the laser pulse. (It is not necessary to measure the radiation emitted by these electrons.) The data collected can be used to distinguish between equations of motion which include or neglect radiation reaction, as they predict different final electron momenta in the experiment. One experimental signal of radiation reaction is the appearance of low energy electrons scattered at angles forbidden by the Lorentz force equation.

Importantly, we have shown that it is possible for the final state of the scattered electrons to be *dominated* by recoil effects, which results in particularly clear signatures of radiation reaction. One such signal would be the reversal of emission direction discussed above, but arranging for this to be visible in a realistic experiment will require considerable fine tuning. The 'generic' signal, namely that the electron emission angle changes due to radiation reaction, is however robust. For long pulses at moderate intensity, for which the transverse focussing is not too tight, the plane wave model should give a reasonably accurate first approximation.

ACKNOWLEDGMENTS

The authors are supported by EPSRC, grant EP/I029206/1-YOTTA (C. H.), the European Research Council, contract 204059-QPQV (A.I. and M.M.), the Swedish Research Council contract 2011-4221 (A.I.), the National Science Foundation under grant PHY-0935197, and the Office of Science of the U.S. Department of Energy under contracts DE-AC02-05CH11231 and DE-FG02-12ER41798.

[1] D. D. Meyerhofer *et al.*, J. Opt. Soc. Am. B **13** (1996) 113; C. I. Moore, J. P. Knauer and D. D. Meyerhofer, Phys. Rev. Lett. **74** (1995) 2439.
[2] C. Harvey, T. Heinzl, A. Ilderton and M. Marklund, Phys. Rev. Lett. **109** (2012) 100402.
[3] K.T. McDonald, arXiv:physics/0003062 [physics.class-ph].
[4] A. Di Piazza, C. Muller, K. Z. Hatsagortsyan and C. H. Keitel, Rev. Mod. Phys. **84** (2012) 1177.
[5] W. P. Leemans, R. Duarte, E. Esarey, S. Fournier, C. G. R. Geddes, D. Lockhart, C. B. Schroeder, C. Toth, J. L. Vay, and S. Zimmermann, AIP Conf. Proc. **1299**, 3 (2010).
[6] M. Tamburini, C. H. Keitel, A. Di Piazza, arXiv:1306.3328 [physics.plasma-ph].
[7] A. Gonoskov, A. Bashinov, I. Gonoskov, C. Harvey, A. Ilderton, A. Kim, M. Marklund and G. Mourou *et al.*, Phys. Rev. Lett. **113** (2014) 014801 [arXiv:1306.5734 [physics.plasm-ph]].
[8] A. G. R. Thomas, C. P. Ridgers, S. S. Bulanov, B. J. Griffin, and S. P. D. Mangles, Phys. Rev. X **2**, 041004 (2012).
[9] A. Ilderton and G. Torgrimsson, Phys. Lett. B **725** (2013) 481.
[10] L. D. Landau and E. M. Lifshitz, *The Classical Theory of Fields (Course of Theoretical Physics, Vol. 2)*, Butterworth-Heinemann, Oxford, 1987.
[11] E.M. McMillan, Phys. Rev. **79**, 498 (1950).
[12] A. L. Troha, J. R. Van Meter, E. C. Landahl, R. M. Alvis, Z. A. Unterberg, K. Li, N. C. Luhmann Jr., A. K. Kerman, F. V. Hartemann, Phys. Rev. E **60**, 926 (1999).
[13] C. Harvey, T. Heinzl and M. Marklund, Phys. Rev. D **84**, 116005 (2011).
[14] H.M. Lai, Phys. Fluids **23**, 2373 (1980).
[15] This is a natural notation since we are looking at the integral of the electric field, but no gauge potential is needed or used.
[16] V. S. Popov, Physics Uspekhi, **47**, 855 (2004).
[17] P. Woodward, J. IEE **93**, 1554 (1946), part IIIA.
[18] P. Woodward and J. Lawson, J. IEE **95**, 363 (1948) part III.
[19] R. Palmer, SLAC-PUB-4320 (1987).
[20] R.H. Pantell and M.A. Piestrup, Appl. Phys. Lett. **32**, 781 (1978).
[21] T. Plettner, R. L. Byer, E. Colby, B. Cowan, C. M. S. Sears, J. E. Spencer and R. H. Siemann, Phys. Rev. Lett. **95**, 134801 (2005).
[22] V. Dinu, T. Heinzl and A. Ilderton, Phys. Rev. D **86** (2012) 085037.
[23] H.A. Lorentz, *The Theory of Electrons*, B.G. Teubner, Leipzig, 1906; reprinted by Dover Publications, New York, 1952 and Cosimo, New York, 2007.
[24] M. Abraham, *Theorie der Elektrizität*, Teubner, Leipzig, 1905.
[25] P.A.M. Dirac, Proc. Roy. Soc. A **167**, 148-169 (1938).
[26] K.T. McDonald, arXiv:physics/0003062v1 [physics.class-ph].
[27] J. Koga, T. Esirkepov and S.V. Bulanov, Phys. Plasma **12**, 093106 (2005).
[28] S. V. Bulanov *et al.*, Nuclear Instruments and Methods in Physics Research A **660** 31 (2011).
[29] S. V. Bulanov, T. Zh. Esirkepov, M. Kando, J. K. Koga, and S. S. Bulanov, Phys. Rev. E **84**, 056605 (2011).
[30] A. Ilderton and G. Torgrimsson, Phys. Rev. D **88** (2013) 025021 [arXiv:1304.6842 [hep-th]].
[31] Y. Kravets, A. Noble and D. Jaroszynski, Phys. Rev. E **88**, 011201(R) (2013).
[32] A. Di Piazza, Lett. Math. Phys. **83**, 305 (2008).

[33] G. Lehmann, and K. H. Spatschek, Phys. Rev. E **84** (2011) 046409.
[34] A. Di Piazza, K. Z. Hatsagortsyan and C. H. Keitel, Phys. Rev. Lett. **102**, 254802 (2009).
[35] One could also utilise large initial gamma factors, $\gamma_i \gg 1$, but this would take us out of the classical regime. This is not the scenario we are pursuing, so we do not discuss this case further.
[36] J. N. Bardsley, B. M. Penetrante and M. H. Mittleman, Phys. Rev. A **40**, 3823 (1989).
[37] F. Mackenroth, A. Di Piazza and C. H. Keitel, Phys. Rev. Lett. **105** (2010) 063903.
[38] N. Neitz, A. Di Piazza, Phys. Rev. Lett. **111**, 054802 (2013).
[39] T. W. B. Kibble, Phys. Rev. **138**, B740 (1965).
[40] V. B. Berestetskii, E. M. Lifshitz and L. P. Pitaevskii, *Quantum Electrodynamics (Course of Theoretical Physics, Vol. 4)*, Pergamon Press, Oxford, 1982.
[41] N. B. Narozhny, and M. S. Fofanov, JETP **90**, 753 (2000).
[42] S. S. Bulanov, N. B. Narozhny, V. D. Mur and V. S. Popov, Phys. Lett. A **330** (2004) 1.
[43] I. Gonoskov, A. Aiello, S. Heugel, and G. Leuchs, Phys. Rev. A **86**, 053836 (2012).
[44] E. Esarey, C. B. Schroeder, and W. P. Leemans, Rev. Mod. Phys. **81**, 1229 (2009).
[45] A. N. Pfeiffer, C. Cirelli, M. Smolarski and U. Keller, Chem. Phys. **414** (2013) 84.
[46] PATRA code: contact S. Rykovanov, Helmholtz Institute Jena, S.Rykovanov@gsi.de.